J|A|C|S
ARTICLES
Published on Web 10/31/2002

Dissociation of CH_3I on the Al(111) Surface − An STM and Density Functional Theory Study

Sergey Mezhenny,[†] Daniel C. Sorescu,[‡,§] Petro Maksymovych,[†] and John T. Yates, Jr.*,[†]

Contribution from the Surface Science Center, Department of Chemistry, University of Pittsburgh, Pittsburgh, Pennsylvania 15260, National Energy Technology Laboratory, U.S. Department of Energy, P.O. Box 10940, Pittsburgh, Pennsylvania 15236, and Department of Chemical and Petroleum Engineering, University of Pittsburgh, Pittsburgh, Pennsylvania 15261

Received June 24, 2002

Abstract: The reaction of methyl iodide with the Al(111) surface was studied by room-temperature scanning tunneling microscopy (STM) and by first principles calculations. It was found that at 300 K methyl iodide decomposes on the Al(111) surface, forming methyl (CH_3), methylidyne (CH), and adsorbed iodine. Methyl groups are observed to occupy atop sites by STM. The occupation of the hollow site by methylidyne was observed in STM measurements. Total energy density functional theory calculations have shown that methyl species occupy atop Al sites (E_A = 45.3 kcal/mol), methylidyne species adsorb on fcc hollow sites (E_A = 155.0 kcal/mol), while individual iodine atoms can bind on both on-top or hollow sites with adsorption energies between 54 and 56 kcal/mol.

I. Introduction

The interaction of the clean Al(111) surface with both inorganic and organic molecules has been studied by many surface science techniques and various theoretical methods.[1−25] However, to the best of our knowledge, only simple adsorption systems such as O/Al(111)[4−7] and H/Al(111)[13,14] have been successfully studied by STM. In contrast, chemical reactions on the transition metal surfaces are well studied,[26,27] and recent STM studies of molecular and atomic adsorbates on these surfaces were summarized in reviews by Besenbacher[28] and Chiang.[29]

Nontransition metal surfaces such as Mg and Al are interesting because of their high reactivity as carbanions. These metals are widely used in organic synthesis,[30] and the mechanism of these "Grignard-type" reactions remains to be investigated at the level of atomic resolution. The surface chemistry of the alkyl halides on Al(111) was first studied using surface science methods by Chen[21] and further studied by Bent[25] and Kondo.[23] It has been found that the halogen atom remains on the surface, while alkyl (R) moieties decompose on the surface.[21,25] The overall reaction, shown in eq 1, produces aluminum sesquihalides[30] by bulk synthesis,[30,31] according to the literature, but studies of the surface show that additional reaction processes occur as a result of the decomposition of the R groups.

$$3RX + 2Al \rightarrow R_2AlX + RAlX_2 \qquad (1)$$

* Corresponding author. E-mail: jyates@pitt.edu.
† Department of Chemistry, University of Pittsburgh.
‡ U.S. Department of Energy.
§ Department of Chemical and Petroleum Engineering, University of Pittsburgh.

(1) Cabrera, N.; Mott, N. F. *Rep. Prog. Phys.* **1948**, *12*, 163.
(2) Zhukov, V.; Popova, I.; Fomenko, V.; Yates, J. T., Jr. *Surf. Sci.* **1999**, *441*, 240.
(3) Zhukov, V.; Popova, I.; Yates, J. T., Jr. *Surf. Sci.* **1999**, *441*, 251.
(4) Brune, H.; Wintterlin, J.; Trost, J.; Ertl, G.; Wiechers, J.; Behm, R. J. *J. Chem. Phys.* **1993**, *99*, 2128.
(5) Trost, J.; Brune, H.; Wintterlin, J.; Behm, R. J.; Ertl, G. *J. Chem. Phys.* **1998**, *108*, 1740.
(6) Schmid, M.; Leonardelli, G.; Tscheliebnig, R.; Biedermann, A.; Varga, P. *Surf. Sci.* **2001**, *478*, L355.
(7) Komrowski, A. J.; Sexton, J. Z.; Kummel, A. C.; Binetti, M.; Weibe, O.; Hasselbrink, E. *Phys. Rev. Lett.* **2001**, *87*, 246103.
(8) Chan, A. W. E.; Hoffmann, R. *J. Vac. Sci. Technol., A* **1991**, *9*, 1569.
(9) Hjelmberg, H. *Surf. Sci.* **1978**, *81*, 539.
(10) Feibelman, P. *Phys. Rev. Lett.* **1992**, *69*, 1568.
(11) Hara, M.; Domen, K.; Onishi, T.; Nozoye, H.; Nishihara, C.; Kaise, Y.; Shindo, H. *Surf. Sci.* **1991**, *242*, 459.
(12) Winkler, A.; Resch, Ch.; Rendulic, K. D. *J. Chem. Phys.* **1991**, *95*, 7682.
(13) Go, E. P.; Thuermer, K.; Reutt-Robey, J. E. *Surf. Sci.* **1999**, *437*, 377.
(14) Go, E. P.; Thuermer, K.; Reutt-Robey, J. E. *J. Phys. Chem. B* **2000**, *104*, 8507.
(15) Russell, J. N., Jr.; Bermudez, V. M.; Leming, A. *Langmuir* **1996**, *12*, 6492.
(16) Russell, J. N., Jr.; Leming, A.; Morris, R. E. *Surf. Sci.* **1998**, *399*, 239.
(17) Shen, W.; Nyberg, G. L. *Surf. Sci.* **1993**, *296*, 49.
(18) Sardar, S. A.; Duschek, R.; Blyth, R. I. R.; Netzer, F. P.; Ramsey, M. G. *Surf. Sci.* **2000**, *468*, 10.
(19) Blyth, R. I. R.; Mittendorfer, F.; Hafner, J.; Sardar, S. A.; Duschek, R.; Netzer, F. P.; Ramsey, M. G. *J. Chem. Phys.* **2001**, *114*, 935.
(20) King, E. M.; Clark, S. J.; Verdozzi, C. F.; Ackland, G. J. *J. Phys. Chem. B* **2001**, *105*, 641.
(21) Chen, J. G.; Beebe, T. P., Jr.; Crowell, J. E.; Yates, J. T., Jr. *J. Am. Chem. Soc.* **1987**, *109*, 1726.
(22) Head, J. D.; Kairys, V.; Shi, Y. *THEOCHEM* **1999**, *464*, 153.
(23) Domen, K.; Kondo, J. N.; Higashi, T.; Yamamoto, H.; Hara, M.; Onishi, T. *Surf. Sci.* **1996**, *349*, 294.
(24) Bent, B. E.; Nuzzo, R. G.; Dubois, L. H. *J. Am. Chem. Soc.* **1989**, *111*, 1634.
(25) Bent, B. E.; Nuzzo, R. G.; Zegarski, B. R.; Dubois, L. H. *J. Am. Chem. Soc.* **1991**, *113*, 1137.
(26) Zaera, F. *Chem. Rev.* **1995**, *95*, 2651.
(27) Bent, B. E. *Chem. Rev.* **1996**, *96*, 1361.
(28) Besenbacher, F. *Rep. Prog. Phys.* **1996**, *59*, 1737.
(29) Chiang, S. *Chem. Rev.* **1997**, *97*, 1083.
(30) Mole, T.; Jeffery, E. A. *Organoaluminum Compounds*; Elsevier: New York, 1972.
(31) Albert, M. R.; Yates, J. T., Jr. *The Surface Scientist's Guide to Organometallic Chemistry*: American Chemical Society: Washington, DC, 1987.

10.1021/ja0208761 CCC: $22.00

As shown earlier by vibrational spectroscopy,[21] CH_3I adsorbs on the Al(111) surface at 150 K as a mixture of undecomposed molecules and the CH(a) and I(a) species. The CH(a) species were identified by a characteristic deformation mode at 760 cm^{-1}; in addition, vibrational modes near 2960 cm^{-1} were attributed to C−H stretching modes of the CH(a) species. These high-frequency modes could not be distinguished from C−H stretching modes of species such as CH_3(a). At 300 K, there is no indication of CH_3I molecular chemisorption. In the work reported here, STM studies at 300 K and first principles calculations were employed to study the surface products of this reaction. High-resolution STM images revealed a mixture of CH_3(a), CH(a), and I(a) on the surface. Theoretical modeling provided the necessary information about the corresponding bonding energies and allowed an unambiguous structural assignment of the STM images.

II. Experimental Section

The experiments were conducted in an ultrahigh vacuum (UHV) system (base pressure $\approx 5 \times 10^{-11}$ Torr) equipped with a room-temperature STM (Omicron), an Auger electron spectrometer (AES, model PHI 15-110), and a quadrupole mass spectrometer (UTI). The Al(111) single crystals (10 mm × 5 mm × 1 mm) were cut from a boule and oriented in an X-ray diffractometer. The crystals were mechanically polished to produce the (111) surface plane orientation (± 0.5°). To remove the surface stress and contaminants introduced by the mechanical polishing, the samples were further electropolished in a mixture of $HClO_4$ (3 mL), 2-butoxyethanol (80 mL), and absolute ethanol (80 mL) at −25 °C ($U = +40$ V, $j = 0.075$ A/cm^2) for 45 s, with the sample at positive potential. In UHV, the samples were cleaned by Ar sputtering cycles ($U_P = 2$ kV, $I_P = 10$ μA) for up to 12 h and annealed at 793 K for 5 min.[2] The sputter cycles were repeated until no oxygen traces were detected by AES.

Tunneling tips were electrochemically etched in KOH solution from 0.25 mm polycrystalline W wire, followed by electron bombardment (500 eV) in UHV. To produce atomic resolution images on the Al(111) surface, a combination of positive and negative voltage pulses was applied while scanning in the STM.[33] All STM images were acquired in the constant current mode. Methyl iodide (Sigma) was purified as described in ref 21 and stored in a glass flask which was wrapped with Al foil to exclude light. Iodine crystals (Sigma) were transferred to a glass storage ampule under a nitrogen atmosphere and additionally purified by several freeze−pump−thaw cycles. The adsorption of CH_3I(g) and I_2(g) was accomplished using a collimated molecular beam doser,[32] which was calibrated for conductance using Ar. The calculated gas flux was corrected for geometrical effects involving the doser−crystal spacing and the dimensions of the doser.[32] During dosing, a methyl iodide flux of 5.9×10^{12} molecules/cm^2 s and an iodine flux of 4.4×10^{12} molecules/cm^2 s have been normally used. The crystal temperature was measured with a K-type thermocouple mounted in a hole drilled into the edge of the crystal. After gas adsorption at 114 K, the crystal was heated in the manipulator up to 300 K before vacuum transfer into the STM.

III. Computational Method

The calculations performed in this study were done using the ab initio total-energy VASP code.[34−36] This program evaluates the total energy of periodically repeating geometries on the basis of density functional theory and the pseudopotential approximation. In this case, only the valence electrons are represented explicitly in the calculations; the electron−ion interaction is described by fully nonlocal optimized ultrasoft pseudopotentials similar to those introduced by Vanderbilt.[37,38] Periodic boundary conditions are used with the occupied electronic orbitals expanded in a plane−wave basis. The expansion includes all plane waves whose kinetic energy $\hbar^2k^2/2m < E_{cut}$, where k is the wave vector, m the electronic mass, and E_{cut} is the chosen cutoff energy. This cutoff energy is chosen to ensure the convergence with respect to the basis set. A cutoff energy of 350 eV has been chosen in these studies. The k-points are obtained from the Monkhorst−Pack scheme.[39] Electron smearing is employed via the Methfessel−Paxton technique,[40] with a smearing width $\sigma = 0.1$ eV. All energies are extrapolated to $T = 0$ K.

The calculations have been done using the spin-polarized Perdew−Wang 91 (PW91) generalized gradient-corrected exchange-correlation functional.[41] Throughout calculations, the total spin of the system has been allowed to relax. The effect of using a different exchange-correlation functional on the adsorption energies has been also investigated by using the Perdew, Burke, and Ernzerhof (PBE) functional[42] as implemented in the commercial version of the software package CASTEP (Cambridge Serial Total Energy Package).[43] The pseudopotentials used in this case are norm-conserving of the form suggested by Kleinman and Bylander[44] and optimized using the scheme of Lin et al.[45] The corresponding cutoff energies were 890 eV for CH_3, CH, and individual C atoms and 450 eV for iodine species, respectively. The optimization of different atomic configurations was performed on the basis of a conjugate-gradient minimization of the total energy.

IV. Results

STM studies of adsorption on metal surfaces require high quality images of the substrate in order to derive correct information about adsorbate site occupancy.[29] Unfortunately, metal surfaces are best imaged at low bias voltages, while adsorbates show higher contrast in the STM images at much higher bias voltages.[29,46] That is why it is important to achieve a compromise in both adsorbate and substrate imaging conditions in order to determine site locations for adsorbed species.

Imaging Reaction Products. It was possible to find large regions of the Al(111) surface free of defects, as shown in Figure 1a. Surface carbon species were found on the Al(111) surface and have been previously studied by STM,[46] X-ray photoelectron diffraction,[47] and theoretical modeling.[48,49] The STM image of two impurity C atoms, shown in Figure 1b, is in a good agreement with previous results.[46] The apparent adsorbate size in the STM image does not usually correspond to the geometry of the adsorbate and is due to electronic effects which can easily affect the neighboring substrate atoms.[50,51] A carbon atom adsorbed in the hollow site is imaged as a slight depression

(32) Winkler, A.; Yates, J. T., Jr. *J. Vac. Sci. Technol., A* **1988**, *6*, 2929.
(33) Wintterlin, J.; Wiechers, J.; Brune, H.; Gritsch, T.; Höfer, H.; Behm, R. J. *Phys. Rev. Lett.* **1989**, *62*, 59.
(34) Kresse, G.; Hafner, J. *Phys. Rev. B* **1993**, *48*, 13115.
(35) Kresse, G.; Furthmüller, J. *Comput. Mater. Sci.* **1996**, *6*, 15.
(36) Kresse, G.; Furthmüller, J. *Phys. Rev. B* **1996**, *54*, 11169.
(37) Vanderbilt, D. *Phys. Rev. B* **1990**, *41*, 7892.
(38) Kresse, G.; Hafner, J. *J. Phys.: Condens. Matter* **1994**, *6*, 8245.
(39) Monkhorst, H. J.; Pack, J. D. *Phys. Rev. B* **1976**, *13*, 5188.
(40) Methfessel, M. Paxton, A. T. *Phys. Rev. B* **1989**, *40*, 3616.
(41) Perdew, J. P.; Chevary, J. A.; Vosko, S. H.; Jackson, K. A.; Pederson, M. R.; Singh, D. J.; Fiolhais, C. *Phys. Rev. B* **1992**, *46*, 6671.
(42) Perdew, J. P.; Burke, K.; Ernzerhof, M. *Phys. Rev. Lett.* **1996**, *77*, 3865.
(43) Milman, V.; Winkler, B.; White, J. A.; Pickard, C. J.; Payne, M. C.; E. V. Akhmatskaya, Nobes, R. H. *Int. J. Quantum Chem.* **2000**, *77*, 895.
(44) Kleinman, L.; Bylander, D. M. *Phys. Rev. Lett.* **1982**, *48*, 1425.
(45) Lin, J. S.; Qteish, A.; Payne, M. C.; Heine, V. *Phys. Rev. B* **1993**, *47*, 4174.
(46) Brune, H.; Wintterlin, J.; Ertl, G.; Behm, R. J. *Europhys. Lett.* **1990**, *13*, 123.
(47) Scalese, S.; Agostino, R. G.; Hayoz, J.; Naumovič, D.; Fasel, R.; Aebi, P.; Schlapbach, L. *Surf. Sci.* **1998**, *395*, 120.
(48) Furthmüller, J.; Kresse, G.; Hafner, J.; Stumpf, R.; Scheffler, M. *Phys. Rev. Lett.* **1995**, *74*, 5084.
(49) Mola, E. E.; Ranea, V. A.; Vicente, J. L. *Surf. Sci.* **1998**, *418*, 367.
(50) Einstein, T. L.; Schrieffer, J. R. *Phys. Rev. B* **1973**, *7*, 3629.
(51) Lang, N. D.; Williams, A. R. *Phys. Rev. B* **1978**, *18*, 616.

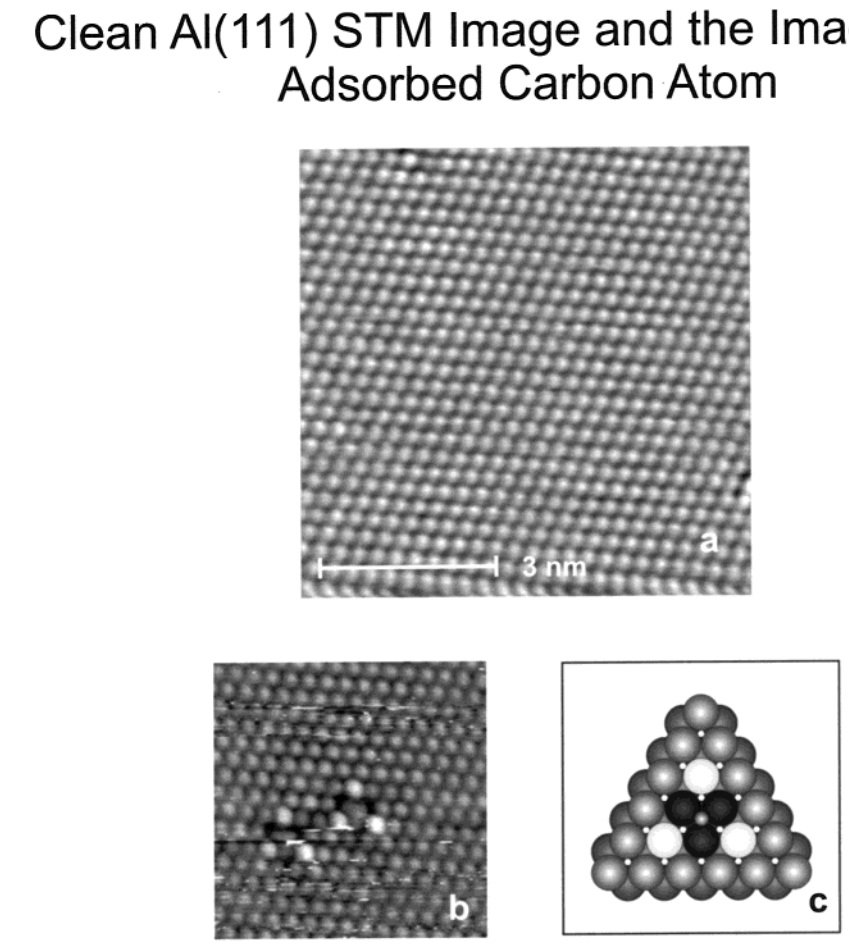

Figure 1. (a) Filled-state STM image ($U = -0.100$ V, $I = 0.366$ nA) of the clean Al(111) surface; (b) filled-state STM image ($U = -0.100$ V, $I = 0.509$ nA) of two C atoms adsorbed on hollow sites; (c) structural model of the C atom adsorbed on the hollow site, according to ref 46.

surrounded by three dark nearest neighbors (nn) and by three next-nearest neighbors (nnn) which appear brighter than the substrate atoms (Figure 1b). A schematic diagram of the STM image for a carbon atom adsorbed in the hollow site is shown in Figure 1c. On the basis of our ability to identify surface carbon atoms, we were able to exclude carbon as a product of CH_3I decomposition on the Al(111) surface.

After imaging the clean surface in the STM, we cooled the sample to $T_S = 114$ K in the manipulator in front of the molecular beam doser. Methyl iodide was dosed on the surface for $t = 180$ s (total fluence $= 1.1 \times 10^{15}$ CH_3I/cm^2), and the sample was then heated to 300 K before transferring it into the STM stage. The STM image from decomposed methyl iodide is shown in Figure 2. Three different types of adsorbate-induced images can be easily distinguished on this large-scale image. Two major image types are attributed to carbon-containing species, and their structures are best seen on the high resolution image, Figure 3. Species I appears in the STM image as six hexagonally arranged bright aluminum atoms, surrounding the central aluminum atom, which is slightly darker than its nearest neighbors, Figure 3a. Species II is centered on a hollow site surrounded by three dark aluminum atoms which are located inside of a nonequilateral hexagon of nine bright aluminum atoms, Figure 3a. The crystallographic location of Species I and II was determined by reference to the Al(111) lattice, as shown by black and white reference circles in Figure 3a. As can be seen from the structural model of these two species shown in Figure 3b and c, Species I is centered at atop Al adsorption site, while Species II is located on a 3-fold hollow site, but the fcc and hcp sites were not distinguished in this work. Both species are immobile at 300 K and no changes were noticed throughout the experiment.

Species III appears as bright low-symmetry immobile clusters of different sizes randomly distributed over the surface. To determine the identity of Species III, a separate experiment was carried out where elementary iodine (I_2) was adsorbed on the Al(111) surface. Previous studies of iodine adsorption on the Al(111) surface[52] have shown that at 300 K the surface coverage is comprised of a majority of Al−I species and a minority of adsorbed AlI_3. The reaction mechanism of iodine monochloride (ICl) with the Al(111) surface was studied in ref 53. Since methyl iodide was adsorbed at $T_S = 114$K, similar experimental conditions were used for iodine adsorption ($T_S = 107$ K, total fluence $= 1.3 \times 10^{15}$ I_2/cm^2). Adsorbed iodine molecules are imaged as a collection of bright clusters randomly distributed over the sample surface, as shown in Figure 4a. There is no evidence of preferential iodine adsorption along the step edge, Figure 4a. Figure 4b shows a high resolution image of the same clusters. It is impossible to distinguish, on the basis of STM images, whether iodine is adsorbed molecularly or dissociatively on the surface. Each individual bright image feature occupies

(52) Jones, R. G.; Fisher, C. J. *Surf. Sci.* **1999**, *424*, 127.
(53) Pettus, K. A.; Taylor, P. R.; Kummel, A. C. *Faraday Discuss.* **2000**, *117*, 321.

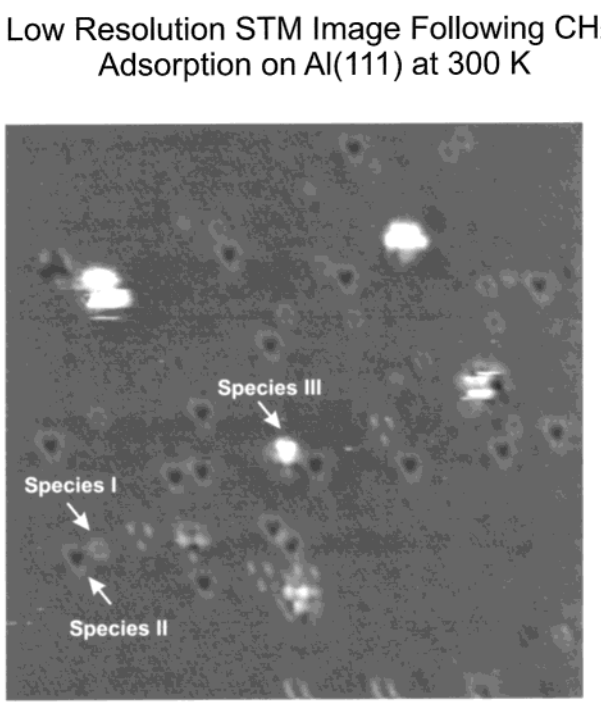

Figure 2. Multiple image types from CH_3I decomposition products (at 300 K) on the Al(111) surface. Filled-state STM image of 25.4 × 25.4 nm^2 ($U = -0.394$ V, $I = 0.299$ nA, total fluence = 2.2×10^{15} CH_3I/cm^2, $T_S = 114$ K).

an area equivalent to approximately four aluminum atoms and does not possess high symmetry (Figure 4b). This can be due to adsorbate−tip interactions during scanning and also due to a large electronic perturbation of the surface by the adsorbate.[50,51] It should be also noted that species from I_2 adsorption are immobile at room temperature. We assign Species III as adsorbed iodine of unknown stoichiometry.

Statistical analysis of the adsorbed species was performed on the large scale STM images, typically up to 30 × 30 nm^2, Figure 2. The ratio between Species I and Species II is close to unity. However, the ratio of the number of Species III to the total number of Species I and Species II is approximately 1:4. This indicates that iodine forms larger clusters rather than individual Al−I(a) adsorbed species. The errors in calculating the number of different species are statistical ($\sigma \approx N^{-0.5}$), and they are not due to a misidentification of different species.

To assign the carbon containing Species I and II and the iodine containing Species III, theoretical calculations were used to determine the adsorption energies and bonding geometries of methyl (CH_3), methylidyne (CH), and iodine atoms adsorbed on the Al(111) surface. The corresponding results are described in the following section.

Results of First Principles Calculations. Preliminary calculations to benchmark the accuracy of our DFT calculations have indicated that a very good agreement is obtained for the prediction of bulk equilibrium crystallographic parameters. For example, from minimizations of the total energy with respect to the volume and shape of the unit cell and to the atomic coordinates within the experimental determined space group symmetry, we have obtained an equilibrium Al lattice constant of 4.044 Å. This value is within 0.1% of the corresponding experimental number of 4.049 Å.

All calculations for the adsorption of various atomic or molecular species on Al(111) surface have been done using a

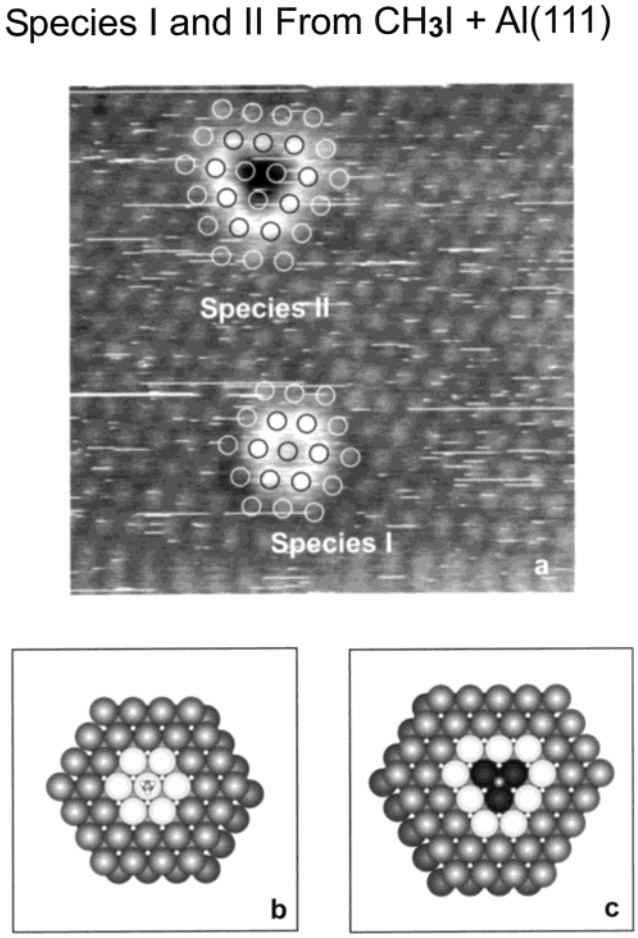

Figure 3. Species assignment. (a) Filled-state STM image of 6 × 6 nm^2 ($U = -0.322$ V, $I = 1.609$ nA) and triangulation diagram locating adsorption sites; proposed site model of (b) adsorbed methyl (Species I) and (c) adsorbed methylidyne (Species II) surface species.

3 × 3 slab with four layers containing 36 Al atoms. For each configuration we studied, the adsorption energy was determined according to eq 2, where E_{ads} is the energy of the adsorbate species, E_{slab} is the total energy of the slab in the absence of the adsorbate, $E_{(ads+slab)}$ is the total energy of the adsorbate/slab system, and N is the number of adsorbate species in the supercell. A positive E_{ads} corresponds to a stable adsorbate/slab system.

$$E_{ads} = (NE_{ads} + E_{slab} - E_{(ads+slab)})/N \qquad (2)$$

The energy of the isolated adsorbate has been determined from calculations in a large simulation box of dimensions 10.0 × 10.5 × 11.0 $Å^3$ and includes spin polarized corrections. The same Brillouin-zone sampling has been used to calculate the energies of the bare slab and of the adsorbate−slab systems.

On the basis of full geometry optimizations of the atomic or molecular species on the Al(111) surface, several major adsorption configurations have been identified. In all these calculations, the top Al layer of the slab has been allowed to relax, while the bottom layers of the slab have been frozen at the bulk optimized configuration. To clarify the nature of the adsorption sites for various species observed in our experimental data, we have focused on the theoretical analysis of the C, CH, CH_3, and iodine species and clusters of iodine atoms adsorbed on the Al(111) surface. A summary of the geometric and energetic parameters

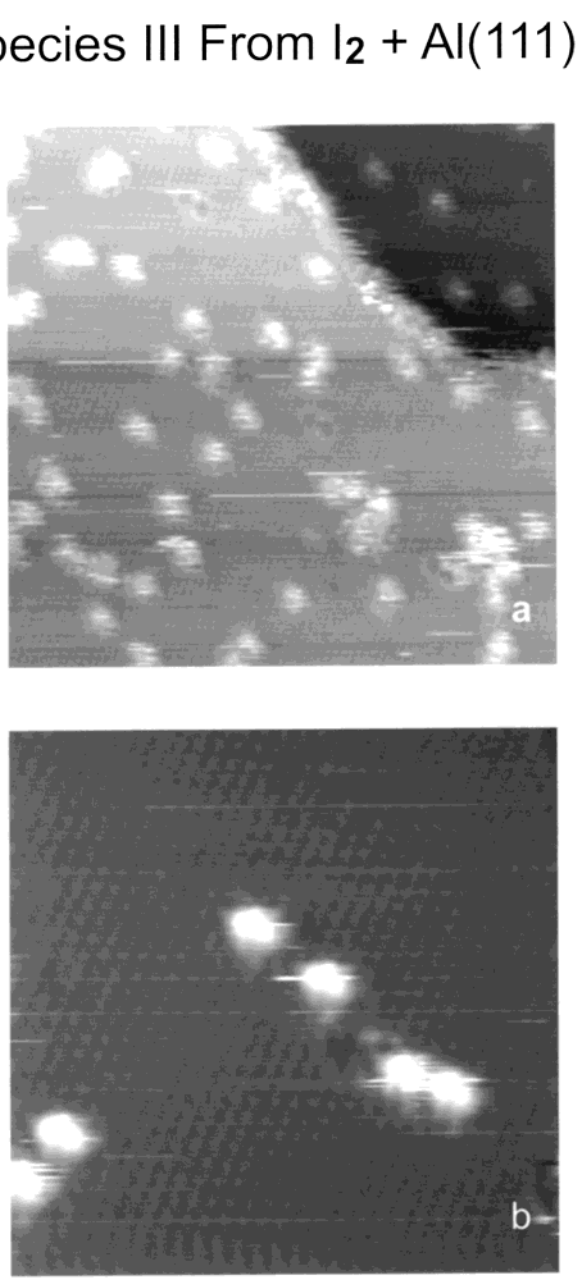

Figure 4. Iodine clusters from I_2 adsorption (at 300 K) on the Al(111) surface (T_S = 107 K, total fluence = 1.3×10^{15} I_2/cm^2). (a) Large scale 25.1×24.9 nm^2 filled-state image ($U = -0.693$ V, $I = 0.322$ nA) and (b) high resolution 10×10 nm^2 filled-state image of the same clusters ($U = -0.500$ V, $I = 0.212$ nA). These images are identical to those images assigned to adsorbed I from CH_3I decomposition.

determined is presented in Table 1. Some representative atomic configurations are depicted in Figure 5 for C, CH, and CH_3 species and in Figure 6 for iodine species and clusters of iodine atoms.

In the case of C isolated atoms, we have determined that the most stable adsorption configurations correspond to the hcp and fcc sites. Dependent on the exchange correlation functional used, the adsorption energies vary between 147 and 151 kcal/mol for PW91 and 149−156 kcal/mol for PBE functionals, respectively. However, independent of the exchange-correlation functional used, the C adsorption at the hollow hcp site is found to be the most stable. In this case, the C atoms actually penetrate into the lattice, as shown in Figure 5a, being positioned slightly below the surface layer. However, the energetic difference between the hcp and fcc sites is relatively small, so both sites should be populated at room temperature. These results confirm the earlier findings determined by Furthmüller et al.[48]

Table 1. Calculated Equilibrium Distances and the Corresponding Adsorption Energies for C, CH, CH_3, and I Species on the Al(111) Surface at Various Sites[a]

	PW91				PBE			
system	$r_{(Al-C)}$	$r_{(C-H)}$	Δh^b	E_{ads}	$r_{(Al-C)}$	$r_{(C-H)}$	Δh	E_{ads}
C: top	1.878			67.5				
hcp	1.908			151.9	1.912			156.0
fcc	1.878			147.3	1.911			149.6
CH: gas phase		1.131						
top	1.804	1.092	−0.287	82.6	1.814	1.083	−0.191	72.3
hcp	1.985	1.101	0.158	147.1	1.974	1.097	0.135	144.3
fcc	1.976	1.098	0.178	155.0	1.962	1.093	0.148	152.3
CH_3: gas phase	1.084							
top	2.001	1.099	0.679	45.3	1.986	1.094	0.629	41.6

system	$r_{(Al-I)}$	E_{ads}	$r_{(Al-I1)}$	E_{ads}
I: top	2.643	60.0	2.620	56.3
hcp	3.084	58.3	3.030	53.9
fcc	3.040	59.1	3.019	54.6

[a] All lengths and energies are given in Å and kcal/mol, respectively. [b] Vertical displacements of the Al atoms involved in binding with a C atom. Positive values refer to displacement toward the vacuum.

For the case of the adsorption of CH_3 species (Species I), we have identified a single adsorption configuration corresponding to an atop site. In this state, the Al−C separation is about 2.0 Å. We also note a significant pull up from the surface toward the vacuum of the Al atom involved in the bonding due to the interaction with a CH_3 radical. Additional calculations started from the adsorption of CH_3 at the other two sites (hollow fcc and hcp sites) and lead to the final adsorption at the atop site. For the atop adsorption configuration of CH_3, the calculated binding energies are 45.3 kcal/mol using PW91 and 41.6 kcal/mol using PBE functionals, respectively.

In the case of CH species (Species II), we have found a stability order E(fcc) > E(hcp) > E(top). The corresponding adsorption energies vary from 155 (152.3) kcal/mol for fcc sites to 82.6 (72.3) kcal/mol for the on-top sites, depending on the type of functionals, PW91 or PBE, used. In the adsorption process, several types of displacements are seen for Al sites involved in bonding. For example, when adsorption takes place on top of an Al atom, this atom is displaced by about −0.2 Å toward the bulk. A reversed type of atomic displacement is seen for the other two adsorption configurations at hcp and fcc sites, where the Al atoms involved in binding move outward toward the vacuum by about 0.15−0.18 Å. On the basis of these results, it can be concluded that the most stable configurations of the CH species correspond to adsorption at fcc hollow site.

Overall, both binding energies found in this study for CH and CH_3 species are smaller than the corresponding energies determined for the isolated Al−CH and Al−CH_3 species.[54] On the basis of ab initio configuration interaction calculations, dissociation energies of 68 kcal/mol for Al−CH_3 and 88 kcal/mol for Al≡CH were determined.

In the case of the isolated iodine atom, we have determined that it can adsorb on the Al(111) surface at distances of about 2.7−3.0 Å from the Al surface atoms (Figure 6 a). As indicated

(54) Fox, D. J.; Ray, D.; Rubesin, P. C.; Schaefer, H. F., III *J. Chem. Phys.* **1980**, *73*, 3246.

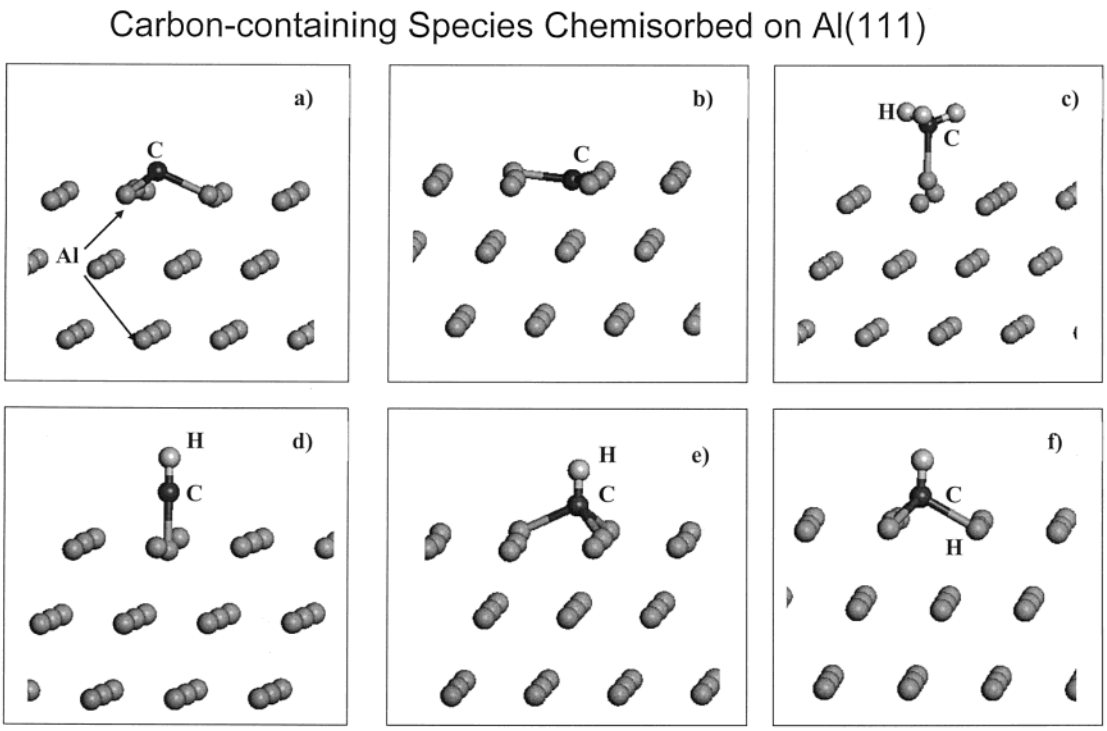

Figure 5. Pictorial view of the equilibrium configurations for isolated C atoms, methyl, and methylidyne adsorbed on the Al(111) surface. (a) C atom on 3-fold hollow hcp site, (b) C atom on 3-fold hollow fcc site, (c) CH_3 on an atop site, (d) CH on an atop site, (e) CH on a 3-fold hollow hcp site, (f) CH on a 3-fold hollow fcc site.

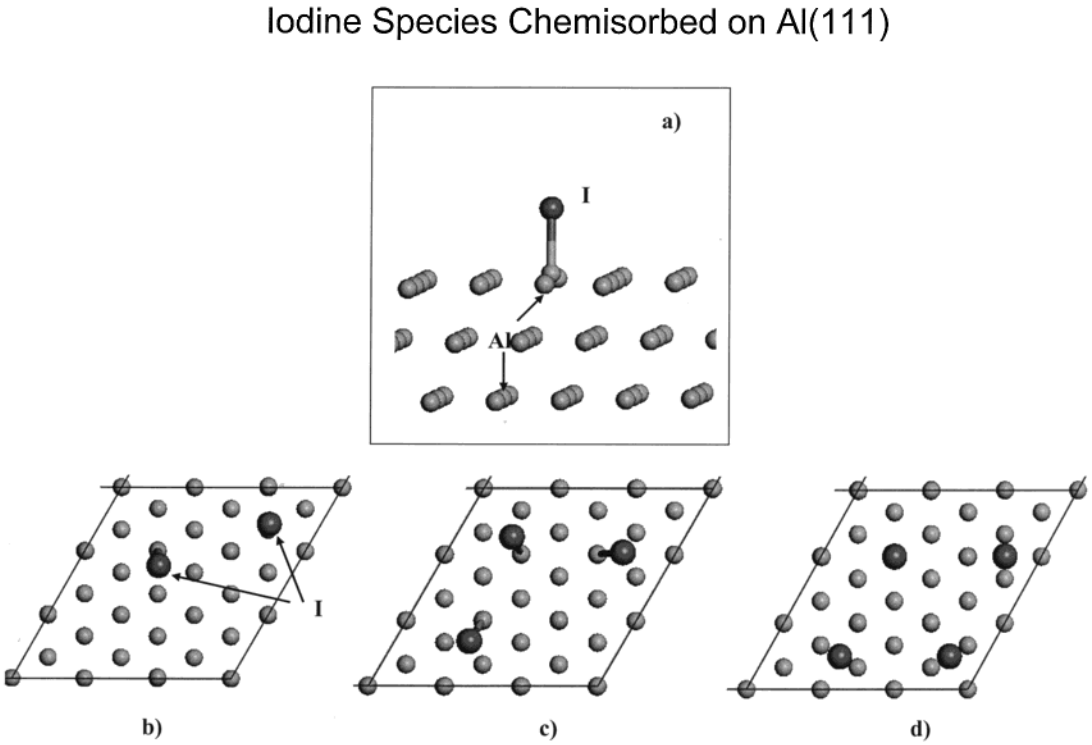

Figure 6. Pictorial view of the calculated equilibrium configuration of the iodine species adsorbed on an atop site (a). Inserts b−d present a top view of the adsorption configurations of iodine atoms placed initially in various configurations on atop sites at two, three, and four neighbor sites.

in Table 1, the corresponding binding energies are very similar for atop, hcp, and fcc sites with values between 58 and 60 kcal/mol or 54 and 56 kcal/mol, depending on whether the PW91 or PBE type of functional is used. These results suggest that all these surface sites can be populated by iodine atoms at room temperature.

As mentioned earlier, the STM images acquired after the adsorption of both CH_3I and I_2 on the Al(111) surface feature bright low-symmetry immobile clusters of different sizes, which were tentatively assigned to clusters of iodine atoms. To investigate the possibility of formation of such clusters theoretically, we have analyzed the case when several iodine atoms (*n*

= 2,4) adsorb at next neighbor sites. In this case, the positions of the iodine atoms on top of the Al surface sites prior to optimization were taken from the results obtained for isolated atom calculations. A pictorial view of the final optimized configurations is given in Figure 6 b−d. Upon adsorption, we find that some of the atoms are displaced from the atop configurations, so that the final lateral separations are 4.6 Å for the $n = 2$ case (Figure 6b), 4.2 Å for the $n = 3$ case (Figure 6c), and 4.3 Å for the $n = 4$ case (Figure 6d). For these configurations, there is a slight variation of the binding energies from 59.1 kcal/mol for the $n = 2$ case to 58.0 kcal/mol for the $n = 4$ structure. The increase of the number of iodine atoms in the supercell to $n = 5$ and $n = 6$ (not shown) leads to a decrease of the lateral I−I separations with a corresponding decrease of the binding energies per iodine atom to 47 kcal/mol for $n = 5$ and 39 kcal/mol for $n = 6$. These results suggest the possibility of iodine cluster formation on Al(111) surface, as also deduced from the STM images.

V. Discussion

Clean Al(111) Surface Imaging by STM. After Al(111) was first successfully imaged in STM with atomic resolution,[32] it was initially suggested by Chen[55] that anomalous corrugation on this surface can be due to the tip W-d_z^2 orbitals, on the basis of the perturbation theory approach. However, tip preparation techniques used to achieve an atomic resolution on the Al(111) surface[32] require certain steps involving strong tip−sample interactions, where either an Al atom or a cluster of Al atoms is transferred to the tip apex. This hypothesis is strongly supported by the recent theoretical calculations performed by Drakova et al.[56] and Hofer et al.[57] Drakova et al.[56] suggest that the high corrugation amplitude is due to the local electron injection into $3p_z$ affinity resonances localized on top of the Al surface atoms. As a result, the system responds dynamically to the charge injection so these levels gain weight near the Fermi level and become dominating in the tunneling process. Hofer et al.[57] found that the tunneling distances necessary to achieve atomic resolution on metal surfaces should be less than 5 Å. However, if the tip−sample separation decreases below 4.5 Å, the probe can become unstable and both tip and sample come into a contact regime. The theoretical findings obtained in these studies are strongly supported by the experimental results. We noted that freshly prepared W tips fail to provide atomic resolution on the Al(111) surface. The resolution can be drastically improved by applying higher biases ($|U| > 3.5$ V) of both polarities while scanning the sample surface.[33] The highest value of the corrugation amplitude obtained on the clean Al(111) surface is about 1.0 Å, Figure 1a, using a bias voltage of $U = -0.1$ V. However, imaging adsorbates with atomic resolution require higher bias voltages (up to $U = -0.9$ V), which leads to a substantial decrease of the corrugation amplitude.[28,34] A corrugation amplitude of about 0.2 Å provides sufficient information necessary to distinguish between different adsorbate structures and to determine their geometrical location on the basis of the image symmetry with respect to the surface lattice, as shown in Figure 3b.

Carbon STM Image. Figure 1b shows the image of a carbon impurity atom which is infrequently observed on the cleaned Al(111) surface. A schematic depiction of the image is shown in Figure 1c. Adsorption of carbon on the 3-fold hcp site is observed. This result is also supported by our theoretical results, which indicate that adsorption at the hollow hcp site is the most stable configuration. The observed STM image is also in agreement with previous work[46,48] and can be clearly differentiated from the images produced by CH_3(a) and CH(a) species. The adsorption of a carbon atom on the 3-fold hcp site leads to lateral electronic interactions which propagate to the next-nearest neighbor sites.

Reaction Products from CH_3I Decomposition on Al(111). Species I and species II (Figure 2) are obtained from the STM imaging of the surface at 300 K after exposure to CH_3I at 114 K. In addition, a species related to iodine adsorption is also observed (Species III), Figure 2.

Species I is centered on an atop Al site, Figure 3a and b. This fact suggests that it should be assigned to CH_3(a) species and that a single C−Al bond would involve an atop site. This assignment is also confirmed by our theoretical calculations, which indicate the existence of stable CH_3 species when adsorbed at the atop site.

Species II is centered on a 3-fold hollow site. It cannot be determined from the experimental STM images we obtained whether this is an hcp site or an fcc site. However, on the basis of our theoretical calculations, it can be concluded that the CH(a) species should be stable and strongly bound to the Al(111) 3-fold fcc hollow site. The presence of CH(a) species on the surface was also demonstrated by the earlier vibrational spectroscopic studies.[21]

The combined STM results and theoretical data suggest the existence of several reaction mechanisms involved in the adsorption of CH_3I on the Al(111) surface. First, both CH_3 and I species can be formed on the surface on the basis of eq 3.

$$CH_3I + (n+1)Al \rightarrow Al{-}CH_3 + Al_nI \ (n = 1 \text{ or } 3) \quad (3)$$

The index n in eq 3 differentiates between the cases when the adsorption of an iodine atom takes place on an atop ($n = 1$) or on a hollow hcp or fcc site ($n = 3$).

In addition, CH species can be formed on the basis of the reaction shown in eq 4, where $n = 1$ or $n = 3$ correspond to the adsorption of an iodine atom on an atop or at a hollow site, respectively.

$$CH_3I + (n+3)Al \rightarrow Al_3CH + Al_nI + H_2(g) \ (n = 1 \text{ or } 3) \quad (4)$$

The evolution of H_2(g) (eq 4) is reported from the work of others.[20,23,24]

Species III comprises a number of bright low-symmetry clusters which are randomly distributed over the surface, as shown in Figure 2. Species such as Al−I(a) and AlI_3 may be involved, although the disturbance of the image by the tip makes a definitive study of Species III impossible. Such an assignment is also supported by our calculations, which indicate that formation of iodine atoms or iodine clusters is possible.

A decidedly non-Boltzmann ratio of Species I (CH_3) to Species II (CH) indicates that the dissociation of CH_3(a) to form CH(a) is controlled kinetically rather than thermodynamically.

(55) Chen, J. C. *Phys. Rev. Lett.* **1990**, *65*, 448.
(56) Drakova, D.; Doyen, G. *Phys. Rev. B* **1997**, *56*, R15577.
(57) Hofer, W. A.; Fisher, A. J.; Wolkow, R. A.; Grütter, P. *Phys. Rev. Lett.* **2001**, *87*, 236104.

The formation of large immobile iodine clusters, which can be formed as a result of the diffusion of individual mobile Al−I species, is strongly supported by the 1:4 ratio of the number of Species III to the total number of Species I and Species II.

VI. Conclusions

Room-temperature STM and theoretical calculations were employed to study the decomposition of methyl iodide on the Al(111) single-crystal surface. The following were determined: (1) At 300 K, only CH_3(a), CH(a), and I(a) species are present on the surface. (2) CH_3(a) and CH(a) are immobile. (3) CH_3(a) adsorbs on an atop Al site with a binding energy of 45.3 kcal/mol, and CH(a) adsorbs on a 3-fold fcc hollow site with a binding energy of 155.0 kcal/mol. These species are easily distinguished from adsorbed C atoms. (4) Iodine atoms can adsorb on an atop or a hollow hcp or fcc site with binding energies of about 54−56 kcal/mol. Additionally, iodine atoms can be present on the surface as clusters.

These results show that the interaction of CH_3I with Al(111) is more complex than would be deduced for the overall reaction (from the literature) shown in eq 1. The CH_3(a) species decomposes to a great extent to produce the CH(a) species. It is likely that the CH(a) species acts to passivate the surface toward further reaction, leading to the product species shown in eq 1.

Acknowledgment. The research was supported by the Army Research Office. The authors would like to thank Drs. Igor Lyubinetsky and Robert Wolkow for helpful discussions.

JA0208761